LFV decays of Z boson in Minimal R-symmetric Supersymmetric Standard Model*

Ke-Sheng Sun(孙科盛)[1;1)] Jian-Bin Chen(陈建宾)[2;2)] Xiu-Yi Yang(杨秀一)[3;3)] Sheng-Kai Cui(崔生恺)[4;4)]

[1]Department of Physics, Baoding University, Baoding 071000, China
[2]College of Physics and Optoelectronic Engineering, Taiyuan University of Technology, Taiyuan 030024, China
[3]School of Science, University of Science and Technology Liaoning, Anshan 114051, China
[4]Department of Physics, Hebei University, Baoding 071002, China

Abstract: A future Z-factory will offer the possibility of studying rare Z decays $Z \to l_1 l_2$, such as those leading to lepton flavor violation (LFV) final states. In this work, by considering the constraints from radiative two-body decays $l_2 \to l_1 \gamma$, we investigate the LFV decays $Z \to l_1 l_2$ in the framework of the Minimal R-symmetric Supersymmetric Standard Model with two benchmark points from the existing literature. The flavor-violating off-diagonal entries δ^{12}, δ^{13} and δ^{23} are constrained by the current experimental bounds of $l_2 \to l_1 \gamma$. Considering recent experimental constraints, we also investigate $\mathrm{Br}(Z \to l_1 l_2)$ as a function of M_D^W. The numerical results show that the theoretical predictions of $\mathrm{Br}(Z \to l_1 l_2)$ in the MRSSM are several orders of magnitude below the current experimental bounds. The LFV decays $Z \to e\tau$ and $Z \to \mu\tau$ may be promising observation targets in future experiments.

Keywords: R-symmetry, MRSSM, lepton flavor violation

PACS: 12.60.Jv, 13.38.Dg, 14.70.Hp **DOI:** 10.1088/1674-1137/43/4/043101

1 Introduction

Rare decays are of a great importance in studying New Physics (NP) beyond the Standard Model (SM); in particular, the lepton-flavor-violation (LFV) decays are appealing because they are suppressed in the SM, and their detection would be a manifest signal of NP. The search for such LFV decays has been pursued to date in a host of processes of leptons, Z boson, Higgs boson, and various hadrons. The present upper bounds on the various LFV decay channels of Z boson from both the LEP data and LHC data is summarized in Table 1 [1]. A pedagogical introduction on the theoretical motivations for charged LFV and the experimental aspects is provided in Ref. [6].

As a new solution to the supersymmetric flavor problem in MSSM, the minimal R-symmetric supersymmetric SM (MRSSM) is proposed in Ref. [7], where the R-symmetry is a fundamental symmetry, which was proposed several decades ago, and is stronger than the R-parity [8, 9]. R-symmetry forbids Majorana gaugino masses, μ term, A terms, and all left-right squark and slepton mass mixings. The R-charged Higgs $SU(2)_L$ doublets $\hat{R}_u$ and $\hat{R}_d$ are introduced in the MRSSM to yield the Dirac mass terms of higgsinos. Additional superfields $\hat{S}$, $\hat{T}$ and $\hat{O}$ are introduced to yield Dirac mass terms of gauginos. Studies on phenomenology in MRSSM can be found in literature [10-23].

In this study, we investigated the LFV decays of Z boson in MRSSM. Similar to the case in MSSM, the LFV decays mainly originate from the off-diagonal entries in slepton mass matrices m_l^2 and m_r^2 [24]. Considering the constraint from radiative decay $l_2 \to l_1 \gamma$ on the off-diagonal parameters, we give the upper predictions on the LFV decays of Z boson with parameter spaces BMP1 and

Received 2 September 2018, Revised 9 January 2019, Published online 1 March 2019

* Supported by the National Natural Science Foundation of China (NNSFC) (11747064, 11805140), the Scientific and Technological Innovation Programs of Higher Education Institutions in Shanxi (2017113), the Foundation of Department of Education of Liaoning province (2016TSPY10) and the Youth Foundation of the University of Science and Technology Liaoning (2016QN11)

1) E-mail: sunkesheng@126.com;sunkesheng@mail.dlut.edu.cn
2) E-mail: chenjianbin@tyut.edu.cn
3) E-mail: yxyruxi@163.com
4) E-mail: 2252953633@qq.com

Table 1. Current limits on LFV decays of Z boson.

decay	bound	experiment	bound	experiment
$Z\to e\mu$	1.7×10^{-6}	LEP (1995) [2]	7.5×10^{-7}	ATLAS (2014) [3]
$Z\to e\tau$	9.8×10^{-6}	LEP (1995) [2]	5.8×10^{-5}	ATLAS (2018) [4]
$Z\to \mu\tau$	1.2×10^{-5}	LEP (1995) [5]	1.3×10^{-5}	ATLAS (2018) [4]

BMP3 [12]. Further, considering recent experimental limit on the masses of charginos and neutrilinos [25], we explore the LFV decays of Z boson as a function of Dirac mass parameter M_D^W. A comparison of the upper bounds of the off-diagonal parameters of the MRSSM and the MSSM is also presented.

The remainder of this paper is organized as follows. In Section 2, we provide a brief introduction on the MRSSM, and we derive the analytic expressions for every Feynman diagram contributing to the LFV decays of Z boson in the MRSSM in detail. The numerical results are presented in Section 3, and the conclusion is provided in Section 4.

2 Formalism

In this section, we first provide a simple overview of the MRSSM. The spectrum of fields in the MRSSM contain the standard MSSM matter; Higgs and gauge superfields augmented by chiral adjoints $\hat{O},\hat{T},\hat{S}$; and two R-Higgs iso-doublets. The superfields with R-charge in the MRSSM are listed in Table 2. The general form of the superpotential of the MRSSM is given by [10]

$$\begin{aligned}\mathcal{W}_{\rm MRSSM} =&\mu_d\left(\hat{R}_d\hat{H}_d\right)+\mu_u\left(\hat{R}_u\hat{H}_u\right)\\&+\Lambda_d\left(\hat{R}_d\hat{T}\right)\hat{H}_d+\Lambda_u\left(\hat{R}_u\hat{T}\right)\hat{H}_u\\&+\lambda_d\hat{S}\left(\hat{R}_d\hat{H}_d\right)+\lambda_u\hat{S}\left(\hat{R}_u\hat{H}_u\right)\\&-Y_d\hat{d}\left(\hat{q}\hat{H}_d\right)-Y_e\hat{e}\left(\hat{l}\hat{H}_d\right)+Y_u\hat{u}\left(\hat{q}\hat{H}_u\right),\end{aligned}\tag{1}$$

where $\hat{H}_u$ and $\hat{H}_d$ are the MSSM-like Higgs weak iso-doublets; $\hat{R}_u$ and $\hat{R}_d$ are the R-charged Higgs $SU(2)_L$ doublets and the corresponding Dirac higgsino mass parameters are denoted as μ_u; and μ_d. λ_u, λ_d, Λ_u and Λ_d are parameters of Yukawa-like trilinear terms involving the singlet $\hat{S}$ and the triplet $\hat{T}$, which is given by

$$\hat{T}=\begin{pmatrix}\hat{T}^0/\sqrt{2} & \hat{T}^+\\ \hat{T}^- & -\hat{T}^0/\sqrt{2}\end{pmatrix}.$$

Then, the soft-breaking terms involving the scalar mass are

$$\begin{aligned}V_{SB,S} =&m_{H_d}^2\left(|H_d^0|^2+|H_d^-|^2\right)+m_{H_u}^2\left(|H_u^0|^2+|H_u^+|^2\right)\\&+\left(B_\mu\left(H_d^-H_u^+-H_d^0H_u^0\right)+h.c.\right)+m_{R_d}^2\left(|R_d^0|^2+|R_d^+|^2\right)\\&+m_{R_u}^2\left(|R_u^0|^2+|R_u^-|^2\right)+m_T^2\left(|T^0|^2+|T^-|^2+|T^+|^2\right)\\&+m_S^2|S|^2+m_O^2|O^2|+\tilde{d}_{L,i}^*m_{q,ij}^2\tilde{d}_{L,j}+\tilde{d}_{R,i}^*m_{d,ij}^2\tilde{d}_{R,j}\\&+\tilde{u}_{L,i}^*m_{q,ij}^2\tilde{u}_{L,j}+\tilde{u}_{R,i}^*m_{u,ij}^2\tilde{u}_{R,j}+\tilde{e}_{L,i}^*m_{l,ij}^2\tilde{e}_{L,j}\\&+\tilde{e}_{R,i}^*m_{r,ij}^2\tilde{e}_{R,j}+\tilde{\nu}_{L,i}^*m_{l,ij}^2\tilde{\nu}_{L,j}.\end{aligned}\tag{2}$$

Note that all trilinear scalar couplings of Higgs bosons, squarks, sleptons, etc. are forbidden owing to the R-symmetry. The Dirac nature is a manifest feature of the MRSSM fermions, and the soft-breaking Dirac mass terms of the singlet $\hat{S}$, triplet $\hat{T}$, and octet $\hat{O}$ take the form

$$V_{SB,DG}=M_D^B\tilde{B}\tilde{S}+M_D^W\tilde{W}^a\tilde{T}^a+M_D^O\tilde{g}\tilde{O}+\text{h.c.},\tag{3}$$

where $\tilde{B}$, $\tilde{W}$, and $\tilde{g}$ are usually MSSM Weyl fermions. After EWSB, one can get the following 4×4 neutralino mass matrix

$$m_{\chi^0}=\begin{pmatrix}M_D^B & 0 & -\frac{1}{2}g_1v_d & \frac{1}{2}g_1v_u\\ 0 & M_D^W & \frac{1}{2}g_2v_d & -\frac{1}{2}g_2v_u\\ -\frac{1}{\sqrt{2}}\lambda_dv_d & -\frac{1}{2}\Lambda_dv_d & -\mu_d^{\rm eff,+} & 0\\ \frac{1}{\sqrt{2}}\lambda_uv_u & -\frac{1}{2}\Lambda_uv_u & 0 & \mu_u^{\rm eff,-}\end{pmatrix},\tag{4}$$

where the modified μ_i parameters are

Table 2. Superfields with R-charge in MRSSM.

field	superfield		boson		fermion	
gauge vector	$\hat{g},\hat{W},\hat{B}$	0	g,W,B	0	$\tilde{g},\tilde{W}\tilde{B}$	+1
matter	$\hat{l},\hat{e}^c$	+1	$\tilde{l},\tilde{e}_R^*$	+1	l,e_R^*	0
	$\hat{q},\hat{d}^c,\hat{u}^c$	+1	$\tilde{q},\tilde{d}_R^*,\tilde{u}_R^*$	+1	q,d_R^*,u_R^*	0
H-Higgs	$\hat{H}_{d,u}$	0	$H_{d,u}$	0	$\tilde{H}_{d,u}$	−1
R-Higgs	$\hat{R}_{d,u}$	+2	$R_{d,u}$	+2	$\tilde{R}_{d,u}$	+1
adjoint chiral	$\hat{O},\hat{T},\hat{S}$	0	O,T,S	0	$\tilde{O},\tilde{T},\tilde{S}$	−1

$$\mu_d^{\text{eff},+} = \frac{1}{2}\Lambda_d v_T + \frac{1}{\sqrt{2}}\lambda_d v_S + \mu_d,$$
$$\mu_u^{\text{eff},-} = -\frac{1}{2}\Lambda_u v_T + \frac{1}{\sqrt{2}}\lambda_u v_S + \mu_u,$$

and v_T and v_S are vacuum expectation values of $\hat{T}$ and $\hat{S}$, respectively, which carry zero R-charge.

The neutralino mass matrix can be diagonalized by unitary matrices N^1 and N^2

$$(N^1)^* m_{\chi^0}(N^2) = \text{diag}(m_{\chi_1^0},...,m_{\chi_4^0}).$$

The chargino mass matrix is given by

$$m_{\chi^\pm} = \begin{pmatrix} g_2 v_T + M_D^W \dfrac{1}{\sqrt{2}}\Lambda_d v_d & \\ \dfrac{1}{\sqrt{2}} g_2 v_d - \dfrac{1}{2}\Lambda_d v_T + \dfrac{1}{\sqrt{2}}\lambda_d v_S + \mu_d & \end{pmatrix}, \quad (5)$$

and it can be diagonalized by unitary matrices U^1 and V^1

$$(U^1)^* m_{\chi^\pm}(V^1) = \text{diag}(m_{\chi_1^\pm}, m_{\chi_2^\pm}).$$

The LFV interactions are mainly caused by the potential misalignment between the leptons and the sleptons mass matrices in the MRSSM. In the gauge eigenstate basis $\tilde{\nu}_{iL}$, the sneutrino mass squared matrix is expressed as

$$m_{\tilde{\nu}}^2 = m_l^2 + \frac{1}{8}(g_1^2 + g_2^2)(v_d^2 - v_u^2) + g_2 v_T M_D^W - g_1 v_S M_D^B, \quad (6)$$

where the last two terms are newly introduced by the MRSSM, and the mass matrix is diagonalized by the unitary matrix Z^V

$$Z^V m_{\tilde{\nu}}^2 (Z^V) = \text{diag}(m_{\tilde{\nu}_1}^2, m_{\tilde{\nu}_2}^2, m_{\tilde{\nu}_3}^2).$$

The slepton mass squared matrix can be expressed as

$$m_{\tilde{L}^\pm}^2 = \begin{pmatrix} (m_{\tilde{L}^\pm}^2)_{LL} & 0 \\ 0 & (m_{\tilde{L}^\pm}^2)_{RR} \end{pmatrix}, \quad (7)$$

where

$$(m_{\tilde{L}^\pm}^2)_{LL} = m_l^2 + \frac{1}{2}v_d^2|Y_e|^2 + \frac{1}{8}(g_1^2 - g_2^2)(v_d^2 - v_u^2) - g_1 v_S M_D^B - g_2 v_T M_D^W,$$
$$(m_{\tilde{L}^\pm}^2)_{RR} = m_r^2 + \frac{v_d^2}{2}|Y_e|^2 + \frac{1}{4}g_1^2(v_u^2 - v_d^2) + 2 g_1 v_S M_D^B.$$

The sources of the LFV are the off-diagonal entries of the 3×3 soft supersymmetry breaking matrices m_l^2 and m_r^2, where the A terms are absent. Note that, in the following, we replace $\tilde{l}$ with $\tilde{L}^\pm$ to denote the sleptons. From Eq. (7), we can see that the left-right slepton mass mixing is also absent. The slepton mass matrix is diagonalized by the unitary matrix Z^E

$$Z^E m_{\tilde{L}^\pm}^2 (Z^E) = \text{diag}\left(m_{\tilde{L}_1^\pm}^2, ..., m_{\tilde{L}_6^\pm}^2\right).$$

The interactions of the charged sleptons $\tilde{L}^\pm$ and neutral sneutrinos $\tilde{\nu}$ with neutralinos χ^0 and charginos $\chi^\pm$ are correspondingly given by the Lagrangian as [12, 26]

$$-i\mathcal{L} = \bar{\chi}_i^0 \left[Y_e^{l_j} N_{i3}^{2*} Z_{k(3+j)}^E P_L + \sqrt{2} g_1 Z_{k(3+j)}^E N_{i1}^1 P_R\right] l_j \tilde{L}_k^\pm + \bar{\chi}^\pm \left[g_2 V_{i1}^{1*} Z_{kj}^V P_L - Z_{kj}^V U_{i2}^1 P_R\right] l_j \tilde{\nu}_k.$$

The interactions between Z boson and neutralinos χ^0 or charginos $\chi^\pm$ are given by the Lagrangian as

$$\begin{aligned} -i\mathcal{L} = & \frac{1}{2}\bar{\chi}_i^\pm \gamma_\mu [\left(2 g_2 c_w V_{j1}^{1*} V_{i1}^1 + (g_2 c_w - g_1 s_w) V_{j2}^{1*} V_{i2}^1\right) P_L \\ & + \left((g_2 c_w - g_1 s_w) U_{i2}^{1*} U_{j2}^1 + 2 g_2 c_w U_{i1}^{1*} U_{j2}^1\right) P_R] \tilde{\chi}_j^\pm Z^\mu \\ & + \frac{1}{2}(g_1 s_w + g_2 c_w) \bar{\chi}_i^0 \gamma_\mu [\left(N_{j4}^{1*} N_{i4}^1 - N_{j3}^{1*} N_{i3}^1\right) P_L \\ & + \left(N_{i4}^{2*} N_{j4}^2 - N_{i3}^{2*} N_{j3}^2\right) P_R] \chi_j^0 Z^\mu. \end{aligned}$$

The relevant Feynman diagrams contributing to the LFV decays of Z boson in the MRSSM is presented in Fig. 1, where Fig. 1(a) and Fig. 1(c) take more important role than others. The Zl_1l_2 interaction Lagrangian can be written as [27]

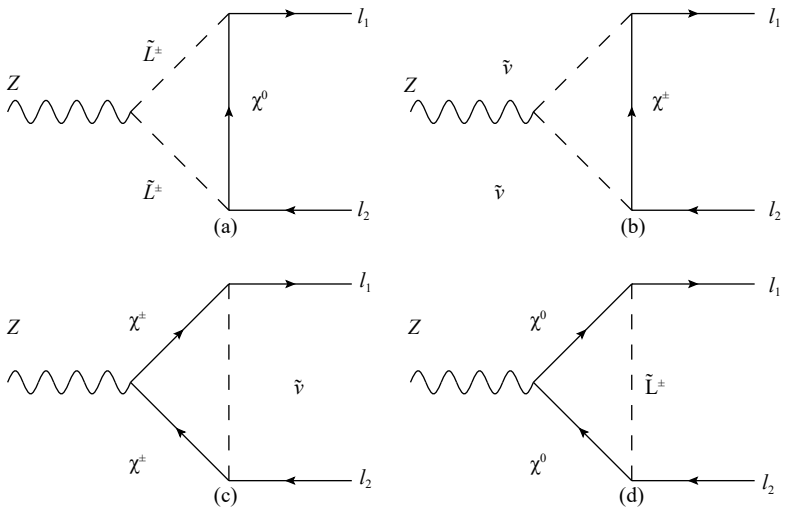

Fig. 1. One loop Feynman diagrams contributing to $Z \to \bar{l}_1 l_2$ in MRSSM.

$$\mathcal{L}_{Zl_1l_2} = \bar{l}_1[\gamma^\mu(C_L^1P_L + C_R^1P_R) + p_1^\mu(C_L^2P_L + C_R^2P_R)]l_2Z_\mu. \quad (8)$$

The left-handed current coefficient C_L^1 for Fig. 1(a) and the right-handed current coefficient C_R^1 for Fig. 1(c) are dominant in the final result. Then the branching ratios of LFV decays of Z boson are calculated using

$$\begin{aligned}\mathrm{Br}(Z\to l_1l_2) =& \mathrm{Br}(Z\to \bar{l}_1l_2) + \mathrm{Br}(Z\to \bar{l}_2l_1)\\ =& \frac{m_Z}{48\pi\Gamma_Z}[2(|C_L^1|^2+|C_R^1|^2) + \frac{m_Z^2}{4}(|C_L^2|^2+|C_R^2|^2)],\end{aligned} \quad (9)$$

where the charged lepton masses have been neglected, and Γ_Z is the total decay width of Z boson. The coefficients $C_{L/R}^1$ and $C_{L/R}^2$ are combinations of coefficients corresponding to each Feynman diagram in Fig. 1 and can be expressed as

$$\begin{aligned}C_{L/R}^1 &= C_{L/R}^{1,a} + C_{L/R}^{1,b} + C_{L/R}^{1,c} + C_{L/R}^{1,d},\\ C_{L/R}^2 &= C_{L/R}^{2,a} + C_{L/R}^{2,b} + C_{L/R}^{2,c} + C_{L/R}^{2,d}.\end{aligned}$$

The coefficients in Fig. 1(a) and Fig. 1(b) can be written as

$$\begin{aligned}C_L^{1,a/b} =& 2C_{1R}C_2C_{3L}C_{00}, C_R^{1,a/b} = 2C_{1L}C_2C_{3R}C_{00},\\ C_L^{2,a/b} =& 2C_2(C_{1L}(C_{3R}m_2 - C_{3L}M_3)C_2 - C_{1L}C_{3L}M_3C_0\\ & - C_{1L}C_{3L}M_3C_1 + C_{1L}C_{3R}m_2C_{22} + C_{1L}C_{3R}m_2C_{12}\\ & + C_{1R}C_{3L}m_1C_{12} + C_{1R}C_{3L}m_1C_{11}\\ & + C_{1R}C_{3L}m_1C_1), C_R^{2,a/b} = C_L^{1,a/b}(L\leftrightarrow R),\end{aligned}$$

where the couplings corresponding to Fig. 1(a) is

$$\begin{aligned}&C_{1L}^{(a)} = -i\sqrt{2}g_1N_{j1}^{1*}Z_{k(3+l_1)}^{E*}, C_{1R}^{(a)} = -iY_e^{l_1}Z_{k(3+l_1)}^{E*}N_{j3}^2,\\ &C_2^{(a)} = i/2\left((g_2c_w - g_1s_w)\sum_{l=1,2,3}Z_{il}^{E*}Z_{kl}^E - 2g_1s_w\sum_{l=1,2,3}Z_{i(3+l)}^{E*}Z_{k(3+l)}^E\right),\\ &C_{3L}^{(a)} = -iY_e^{l_2}N_{j3}^{2*}Z_{i(3+l_2)}^E, \quad C_{3R}^{(a)} = -i\sqrt{2}g_1Z_{i(3+l_2)}^EN_{j1}^1,\\ &M_1 = m_{\tilde{L}_k^\pm}, \quad M_2 = m_{\tilde{L}_i^\pm}, \quad M_3 = m_{\chi_j^0},\end{aligned}$$

and the couplings corresponding to Fig. 1(b) are

$$\begin{aligned}&C_{1L}^{(b)} = iY_e^{l_1}U_{j2}^{1*}Z_{kl_1}^{V*}, \quad C_{1R}^{(b)} = -ig_2Z_{kl_1}^{V*}V_{j1}^1, \quad C_2^{(b)} = -i/2(g_2c_w + g_1s_w),\\ &C_{3L}^{(b)} = -ig_2Z_{il_2}^VV_{j1}^{1*}, \quad C_{3R}^{(b)} = iY_e^{l_2}U_{j2}^1Z_{il_2}^V, \quad M_1 = m_{\tilde{\nu}_k}, \quad M_2 = m_{\tilde{\nu}_i}, \quad M_3 = m_{\chi_j^+}.\end{aligned}$$

The coefficients in Fig. 1(c) and Fig. 1(d) can be expressed as

$$\begin{aligned}C_L^{1,c/d} =& C_{1R}C_{2L}C_{3L}\mathcal{B}_0 - m_2C_0(C_{1L}C_{2L}C_{3R}m_1 + C_{1R}(C_{2L}C_{3R}M_1 - C_{2R}C_{3L}m_2 + C_{2R}C_{3R}M_2)) - C_{1R}C_{2L}C_{3R}M_1m_2C_0\\ & + C_{1R}C_{2R}C_{3L}M_3^2C_0 - 2C_{1R}C_{2R}C_{3L}C_{00} + C_{1L}C_{2L}C_{3L}m_1M_2C_0 - C_{1L}C_{2L}C_{3R}m_1m_2C_0 + C_{1R}C_{2L}C_{3L}M_1M_2C_0\\ & + m_1C_1(C_{1L}(C_{2L}C_{3L}M_2 - C_{2L}C_{3R}m_2 + C_{2R}C_{3L}M_1) + C_{1R}C_{2R}C_{3L}m_1), C_R^{1,c/d} = C_L^{1,c/d}(L\leftrightarrow R), C_R^{2,c/d}\\ =& C_L^{2,c/d}(L\leftrightarrow R), C_L^{2,c/d} = 2(C_{1L}C_{2L}(C_{3L}M_2 - C_{3R}m_2)C_2 - C_{1L}C_{2L}C_{3R}m_2C_{22} - C_{1L}C_{2L}C_{3R}m_2C_{12} - (C_{1L}M_1\\ & + C_{1R}m_1)C_{2R}C_{3L}C_1 - C_{1R}C_{2R}C_{3L}m_1C_{12} - C_{1R}C_{2R}C_{3L}m_1C_{11}),\end{aligned}$$

where the couplings corresponding to Fig. 1(c) is

$$\begin{aligned}&C_{1L}^{(c)} = iY_e^{l_1}U_{k2}^{1*}Z_{jl_1}^{V*}, \quad C_{1R}^{(c)} = -ig_2Z_{jl_1}^{V*}V_{k1}^1,\\ &C_{2L}^{(c)} = -i/2((g_2c_w - g_1s_w)V_{i2}^{1*}V_{k2}^1 + 2g_2c_wV_{i1}^{1*}V_{k1}^1), \quad C_{3L}^{(c)} = -ig_2Z_{jl_2}^VV_{i1}^{1*},\\ &C_{2R}^{(c)} = -i/2((g_2c_w - g_1s_w)U_{k2}^{1*}U_{i2}^1 + 2g_2c_wU_{k1}^{1*}U_{i1}^1), \quad C_{3R}^{(c)} = iY_e^{l_2}U_{i2}^1Z_{jl_2}^V,\\ &M_1 = m_{\chi_k^+}, \quad M_2 = m_{\chi_i^+}, \quad M_3 = m_{\tilde{\nu}_j},\end{aligned}$$

and the couplings corresponding to Fig. 1(d) is

$$\begin{aligned}&C_{1L}^{(d)} = -i\sqrt{2}g_1N_{k1}^{1*}Z_{j(3+l_1)}^{E*}, \quad C_{1R}^{(d)} = -iY_e^{l_1}Z_{j(3+l_1)}^{E*}N_{k3}^2,\\ &C_{2L}^{(d)} = i/2(g_2c_w + g_1s_w)(N_{i3}^{1*}N_{k3}^1 - N_{i4}^{1*}N_{k4}^1), \quad C_{3L}^{(d)} = -iY_e^{l_2}N_{i3}^{2*}Z_{j(3+l_2)}^E,\\ &C_{2L}^{(d)} = i/2(g_2c_w + g_1s_w)(N_{k3}^{2*}N_{i3}^2 - N_{k4}^{2*}N_{i4}^2), \quad C_{3R}^{(d)} = -i\sqrt{2}g_1Z_{j(3+l_2)}^EN_{i1}^1,\\ &M_1 = m_{\chi_k^0}, \quad M_2 = m_{\chi_i^0}, \quad M_3 = m_{\tilde{L}_j^\pm}.\end{aligned}$$

The above loop integrals can be given in the terms of Passarino-Veltman functions [28]

$$\begin{aligned}\mathcal{B}_0 &= \frac{i}{16\pi^2}\mathcal{B}_0\left(m_Z^2, M_1, M_2\right),\\ C_{1,2,\ldots} &= \frac{i}{16\pi^2}C_{1,2,\ldots}\left(m_1^2, m_Z^2, m_2^2; M_3, M_1, M_2\right),\end{aligned}$$

and they can be calculated by the Mathematica package Package-X [29] through a link to fFortran library Collier [30-33], where the latter provides the numerical evaluation of one-loop scalar and tensor integrals in perturbative relativistic quantum field theories.

3 Numerical analysis

In the numerical analysis, we use the benchmark

points in Ref. [12] as the default values for our parameter setup; the points are displayed in Table 3. In the table, the slepton mass matrices are diagonal, and all mass parameters are in GeV or GeV^2. The mass spectra for the BMPs are summarized in Table 4. Note that large values of $|v_T|$ are excluded by the measurement of W mass because the vev v_T of the $SU(2)_L$ triplet field T^0 gives a correction to W mass using [10]

Table 3. Benchmark points.

input	tanβ	λ_d,λ_u	Λ_d,Λ_u	v_S	v_T	M_D^B	M_D^W	μ_d,μ_u	m_T^2	m_l^2,m_r^2
BMP1	3	1.0,−0.8	−1.0,−1.2	5.9	−0.33	600	500	400,400	3000^2	1000^2,1000^2
BMP3	40	0.15,−0.15	−1.0,−1.15	−0.14	−0.34	250	500	400,400	3000^2	1000^2,1000^2

Table 4. Spectrum of different BMPs in GeV.

input	H_1	H_2	A_1	$H_1^\pm$	χ_1^0	χ_2^0	$\chi_1^\pm$	$\tilde{\nu}$
BMP1	125.3	897	896	899	415	420	416	1002
BMP3	125.1	1245	1245	1248	251	408	408	1000

$$m_W^2 = \frac{1}{4}g_2^2(v_u^2+v_d^2)+g_2^2v_T^2. \tag{10}$$

To decrease the number of free parameters involved in our calculation, we assume that the diagonal entries of two 3×3 matrices m_l^2 and m_r^2 are equal $(m_l^2)_{II}=(m_r^2)_{II}$, which is similar to the values shown in Table 3, where $I=$ 1, 2, 3. Then, the only sources of LFV are off-diagonal entries of the soft breaking terms m_l^2, m_r^2, which are parameterized the by mass insertion, as in [34]

$$(m_l^2)^{IJ}=\delta_l^{IJ}\sqrt{(m_l^2)^{II}(m_l^2)^{JJ}},$$
$$(m_r^2)^{IJ}=\delta_r^{IJ}\sqrt{(m_r^2)^{II}(m_r^2)^{JJ}},$$

where $I, J=1, 2, 3$. We also assume $\delta_l^{IJ}=\delta_r^{IJ}=\delta^{IJ}$. The experimental limits on LFV decays, such as radiative two body decays $l_2\to l_1\gamma$, leptonic three body decays $l_2\to 3l_1$, and $\mu-e$ conversion in nuclei can give strong constraints on the parameters δ^{IJ}. In the following, we will use LFV decays $l_2\to l_1\gamma$ to constrain the parameters δ^{IJ}. Current limits of the LFV decays $l_2\to l_1\gamma$ listed in Table 5 [1].

The sparticle mediated diagrams for $l_2\to l_1\gamma$ in MRSSM are shown in Fig. 2. Considering the gauge invariance, and assuming the photon is on shell and transverse, the amplitude for $l_2\to l_1\gamma$ is given by [37]

$$M(l_2\to l_1\gamma)=\epsilon^{\mu*}\bar{u}_{l_1}(p_{l_1})[iq^\nu\sigma_{\mu\nu}(A+B\gamma_5)]u_{l_2}(p_{l_2}). \tag{11}$$

Then, in the limit $m_1\to 0$, the analytic expression of Br$(l_2\to l_1\gamma)$ is derived as

$$\mathrm{Br}(l_2\to l_1\gamma)=\frac{m_{l_2}^3}{8\pi\Gamma_{l_2}}(|A|^2+|B|^2), \tag{12}$$

where Γ_{l_2} is the total decay width of l_2, and the form factors A and B are a combination of the form factors for every Feynman diagram in Fig. 2,

$$A=A^{(a)}+A^{(b)}, B=B^{(a)}+B^{(b)}.$$

In the limit $m_1\to 0$, the form factors $A^{(a)}$ and $B^{(a)}$ corresponding to Fig. 2(a) are given as

$$\begin{aligned}A^{(a)}=&-\frac{i}{32\pi^2}[m_2(C_{1L}C_{2L}C_{3R}+C_{1R}C_{2R}C_{3L})(C_{12}+C_{11})+M_1(C_{1L}C_{2R}C_{3L}+C_{1R}C_{2L}C_{3R})C_2\\&+(M_2(C_{1L}C_{2L}C_{3L}+C_{1R}C_{2R}C_{3R})+m_2(C_{1L}C_{2L}C_{3R}+C_{1R}C_{2R}C_{3L}))C_1],\\B^{(a)}=&\frac{i}{32\pi^2}[M_1(C_{1L}C_{2R}C_{3L}-C_{1R}C_{2L}C_{3R})C_2-m_2(C_{1R}C_{2R}C_{3L}-C_{1L}C_{2L}C_{3R})(C_{12}\\&+C_{11})+(C_{1L}C_{2L}(M_2C_{3L}+m_2C_{3R})-C_{1R}C_{2R}(M_2C_{3R}+m_2C_{3L}))C_1],\end{aligned}$$

and the form factors $A^{(b)}$ and $B^{(b)}$ corresponding to Fig. 2(b) are given as

$$\begin{aligned}A^{(b)}=&-\frac{iC_2}{64\pi^2}[M_3(C_{1L}C_{3L}+C_{1R}C_{3R})(C_0+2C_1+2C_2)-m_2(C_{1L}C_{3R}+C_{1R}C_{3L})(2C_{12}+2C_{11}+C_1)],\\B^{(b)}=&\frac{iC_2}{64\pi^2}[M_3(C_{1L}C_{3L}-C_{1R}C_{3R})(C_0+2C_1+2C_2)-m_2(C_{1L}C_{3R}-C_{1R}C_{3L})(2C_{12}+2C_{11}+C_1)],\end{aligned}$$

where the loop integrals $C_{1,2,\ldots}$ denote $\frac{i}{16\pi^2}C_{1,2,\ldots}(m_2^2,0,0;M_3,M_2,M_1)$. The couplings corresponding to Fig. 2(a) are given as

$$C^{(a)}_{1L} = iY^{l_1}_e U^{1*}_{i2} Z^V_{kl_1}, \quad C^{(a)}_{1R} = -ig_2 Z^{V*}_{kl_1} V^1_{i1}, \quad C^{(a)}_{2L} = C^{(a)}_{2R} = -ie\delta_{ij},$$
$$C^{(a)}_{3L} = -ig_2 V^{1*}_{j1} Z^V_{kl_2}, \quad C^{(a)}_{3R} = iY^{l_2}_e U^1_{j2} Z^V_{kl_2}, \quad M_1 = m_{\chi^+_i}, \quad M_2 = m_{\chi^+_j}, \quad M_3 = m_{\tilde{\nu}_k}.$$

and the couplings corresponding to Fig. 2(b) are given as

$$C^{(b)}_{1L} = -i\sqrt{2}g_1 N^{1*}_{k1} Z^{E*}_{i(3+l_1)}, \quad C^{(b)}_{1R} = -iY^{l_1}_e Z^{E*}_{i(3+l_1)} N^2_{k3}, \quad C^{(b)}_{3L} = -iY^{l_2}_e N^{2*}_{k3} Z^E_{j(3+l_2)},$$
$$C^{(b)}_2 = ie\delta_{ij}, \quad C^{(b)}_{3R} = -i\sqrt{2}g_1 Z^E_{j(3+l_2)} N^1_{k1}, \quad M_1 = m_{\tilde{L}^\pm_i}, \quad M_2 = m_{\tilde{L}^\pm_j}, \quad M_3 = m_{\chi^0_k}.$$

Table 5. Current limits of LFV decays of $l_2 \to l_1\gamma$.

decay	bound	experiment	decay	bound	experiment
$\mu \to e\gamma$	4.2×10^{-13}	MEG(2016) [35]	$\tau \to e\gamma$	3.3×10^{-8}	BABAR(2010) [36]
$\tau \to \mu\gamma$	4.4×10^{-8}	BABAR(2010) [36]	–	–	–

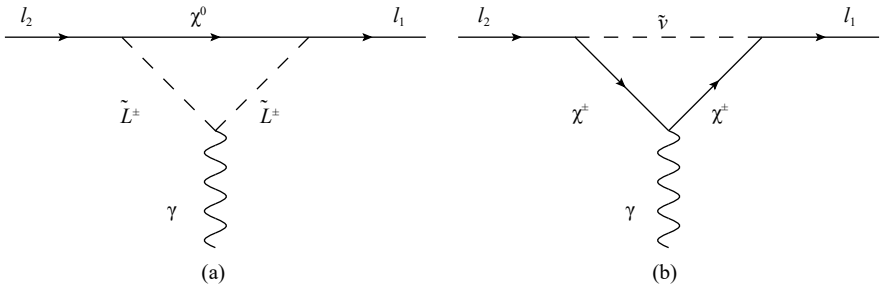

Fig. 2. Feynman diagrams contributing to the LFV decays $l_2 \to l_1\gamma$ in MRSSM.

Taking $\delta^{13} = 0$, $\delta^{23} = 0$, we plot the theoretical prediction of Br $(\mu \to e\gamma)$ versus δ^{12} and Br$(Z \to e\mu)$ versus δ^{12} in Fig. 3(a) and Fig. 3(b), where the horizontal dotted line is the current experimental bounds of Br$(\mu \to e\gamma)$. The solid line denotes the result calculated with parameter setup BMP1, and the dashed line denotes the result calculated with parameter setup BMP3. A linear relationship is displayed between Br$(\mu \to e\gamma)$ or Br$(Z \to e\mu)$ and the flavor violating parameter δ^{12}. The prediction on Br$(\mu \to e\gamma)$ exceeds the current experiment limit at $\delta^{12} \sim 1.0\times10^{-3}$. The parameter space of δ^{12} would have been highly suppressed below $O(10^{-3})$ by considering the future sensitivity of the experiment, which is Br$(\mu \to e\gamma) \sim 6\times10^{-14}$ [38]. The current prediction of Br$(Z \to e\mu)$ in MRSSM is around$O(10^{-13})$, and this prediction is six orders of magnitude below the current limit $O(10^{-7})$. Based on the flavour expansion theorem, various LFV processes have been investigated in MSSM using a recently developed technique which performs a purely algebraic mass-insertion expansion of the amplitudes [39]. Considering the constraints from radiative charged lepton decays, upper bounds on the flavor violating parameters δ^{12}_l (Δ^{21}_{LL}) and δ^{12}_r (Δ^{21}_{RR}) are given in Ref. [39] with $\delta^{12}_l \sim 8.4\times10^{-4}$ (tanβ = 2) and $\delta^{12}_r \sim 5.0\times10^{-3}$ (tanβ = 2). It shows that flavor violating μ lepton decays still provide the most stringent bounds on supersymmetric effects.

Taking $\delta^{12} = 0$, $\delta^{23} = 0$, we plot the theoretical prediction of Br $(\tau \to e\gamma)$ versus δ^{13} and Br$(Z \to e\tau)$ versus δ^{13} in Fig. 3(d) and Fig. 3(d), where the horizontal dotted line is the current experimental bounds of Br$(\tau \to e\gamma)$. The solid line denotes the result calculated with parameter setup BMP1, and the dashed line denotes the result calculated with parameter setup BMP3. Both predictions on Br$(\tau \to e\gamma)$ and Br$(Z \to e\tau)$ decrease as the flavor violating parameter δ^{13} varies from 0.9 to 0.1. The prediction on Br$(\tau \to e\gamma)$ exceeds the current experiment limit at $\delta^{13} \sim 0.75$. Considering the future experimental expectation on Br$(\tau \to e\gamma)$, which is approximately 2.3×10^{-9} [40], the parameter space of δ^{13} would have been suppressed below 0.3. The upper theoretical prediction on Br$(Z \to e\tau)$ in MRSSM is around $O(10^{-8})$, and this prediction is two orders of magnitude below the current limit $O(10^{-6})$. Recent upper bounds on the flavor violating parameters δ^{13}_l (Δ^{31}_{LL}) and δ^{13}_r (Δ^{31}_{RR}) in MSSM are given by $\delta^{13}_l \sim 4.6\times10^{-1}$ (tanβ=2) and $\delta^{13}_r \sim O(1)$ (tanβ=2) [39].

Taking $\delta^{12} = 0$, $\delta^{13} = 0$, we plot the theoretical prediction of Br $(\tau \to \mu\gamma)$ versus δ^{23} and Br$(Z \to \mu\tau)$ versus δ^{23} in Fig. 3(e) and Fig. 3(f), where the horizontal dotted line is the current experimental bounds of Br$(\tau \to \mu\gamma)$. The solid line denotes the result calculated with parameter setup BMP1, and the dashed line denotes the result calculated with parameter setup BMP3. Both predictions on Br$(\tau \to \mu\gamma)$ and Br$(Z \to \mu\tau)$ decrease sharply as the flavor violating parameter δ^{13} is close to 0.1. The prediction

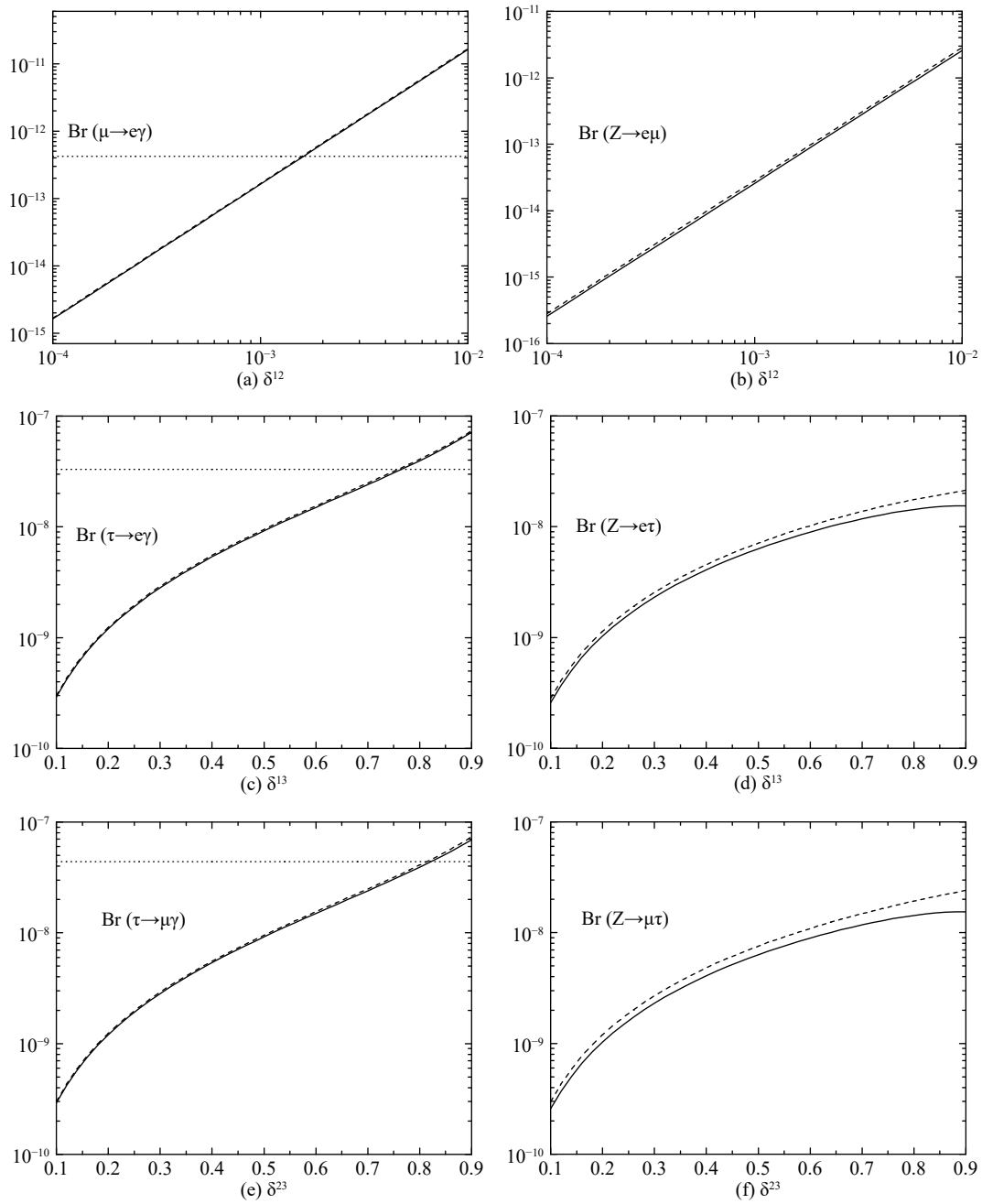

Fig. 3. (a) Br($\mu \to e\gamma$) versus δ^{12}; (b) Br($Z \to e\mu$) versus δ^{12}; (c) Br($\tau \to e\gamma$) versus δ^{13}; (d) Br($Z \to e\tau$) versus δ^{13}; (e) Br($\tau \to \mu\gamma$) versus δ^{23}; (f) Br($Z \to \mu\tau$) versus δ^{23}. The horizontal dotted line in the left panel denotes the current experimental bounds. The solid line denotes the result with BMP1, and the dashed line denotes the result with BMP3.

on Br($\tau \to \mu\gamma$) exceeds the current experiment limit at $\delta^{23} \sim 0.8$. Considerng the future experimental expectation on Br($\tau \to \mu\gamma$), which is approximately (1.8×10^{-9}) [40], the parameter space of δ^{23} would have also been suppressed below 0.3. The upper theoretical prediction on Br($Z \to \mu\tau$) in MRSSM is also around $O(10^{-8})$, and this prediction is three orders of magnitude below the current limit $O(10^{-5})$. Recent upper bounds on the flavor violating parameters δ_l^{23} (Δ_{LL}^{32}) and δ_r^{23} (Δ_{RR}^{32}) in MSSM are given by $\delta_l^{23} \sim 5.3 \times 10^{-1}(\tan\beta{=}2)$ and $\delta_r^{23} \sim O(1)\,(\tan\beta{=}2)$ [39].

Recently, the ATLAS collaboration has released a search for chargino-neutralino production in two and three lepton final states, employing RJR techniques that target specific event topologies [25], which state that charginos and neutralinos must be heavier than 600 GeV at 95% CL. To be compatible with the experimental limit, the parameters M_D^W, M_D^B, μ_u, and μ_d, which dominant the masses of charginos and neutralinos, should be enlarged.

The selection of BMP1 and BMP3 is shown in Fig.8.2 in Ref. [41], where the parameters are set to BMP1 and BMP3 for the top and bottom row, respectively, and the benchmark point is marked by a star in each plot. It is shown that the valid region is $\mu_u(\mu_d) <$ 500 GeV for BMP1, and this leads to at least two sparticle mass lighter than 600 GeV. For BMP3, the valid region for $\mu_u(\mu_d)$ can be enlarged above 600 GeV along with M_D^W and M_D^B. Then, to quantitatively study the LFV decays of Z boson, we perform a scan under BMP3 over the parameters M_D^W and M_D^B, with $\mu_u(\mu_d)$ = 600 GeV. The ranges of the variation over the MRSSM parameters are displayed in Table 6; all mass parameters are in GeV. Moreover, the three flavor violating parameters δ^{12}= 10^{-3}, δ^{13} =0.3, and δ^{23} =0.3 are assumed.

Over a general scan of thousands of points in parameter spaces according to Table 6, we display the predictions on Br($Z \to e\mu$), Br($Z \to e\tau$), and Br($Z \to \mu\tau$) as a function of M_D^W in Fig. 4(a), (b), and (c), respectively. It shows that the predictions on Br($Z \to e\mu$), Br($Z \to e\tau$), and Br($Z \to \mu\tau$) decrease as M_D^W varies from 600 GeV to 800 GeV. For Br($Z \to e\mu$), the range of the prediction is narrowed above $O(10^{-14})$ at M_D^W =600 GeV, and narrowed to $O(10^{-15} - 10^{-14})$ at M_D^W=800 GeV. For Br($Z \to e\tau$) and Br($Z \to \mu\tau$), the range of the prediction is narrowed above $O(10^{-9})$ at M_D^W =600 GeV and $O(10^{-10} - 10^{-9})$ at M_D^W =800 GeV.

Table 6. Range of input parameters for the numerical scan with BMP3.

parameter	Min	Max	step
M_D^W	600	800	10
M_D^B	600	1000	10

4 Conclusions

In this work, considering the constraints on the parameter space from radiative charged lepton decays Br($l_2 \to l_1\gamma$), we analyzed the LFV decays of $Z \to l_1 l_2$ as a function of the flavor violating off-diagonal entries δ^{12}, δ^{13} and ,δ^{23} in the framework of the MRSSM. A summary on the upper limits on flavor violating parameters in MRSSM is provided in Table 7, where the results in MSSM are also included for reference. It shows that the upper limits for two different models are very close to each other.

The LFV decays of $Z \to l_i l_j$ depend strongly on the three flavor violating parameters δ^{ij} in soft breaking terms m_l and m_r, i.e., if set $\delta_{ij} = 0$, then the branching ra-

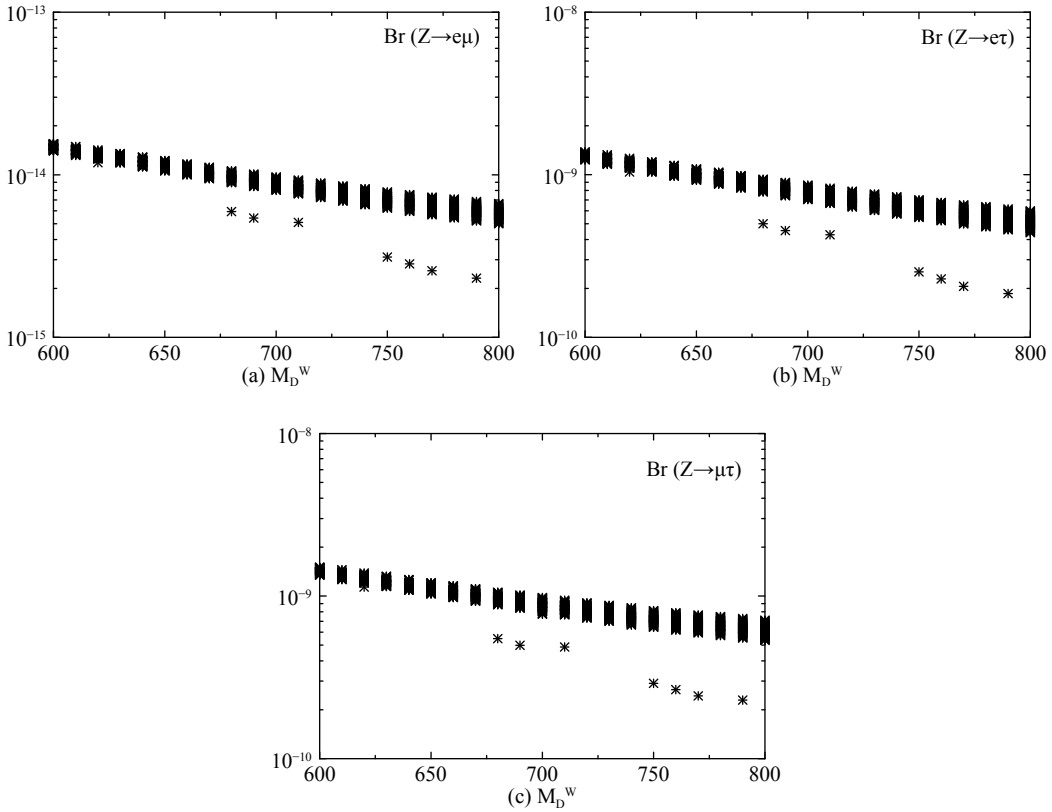

Fig. 4. (a) Br($Z \to e\mu$) versus M_D^W; (b) Br($Z \to e\tau$) versus M_D^W; (c) Br($Z \to \mu\tau$) versus M_D^W. All points satisfy the experimental bound in Table 5.

Table 7. Upper limits on off-diagonal entries δ^{12}, δ^{13} and δ^{23}.

parameters	MRSSM	MSSM($\Delta^{IJ}_{LL}/\Delta^{IJ}_{RR}$ [39])
δ^{12}	1.0×10^{-3}	$8.4\times10^{-4}/5.0\times10^{-3}$
δ^{13}	3.0×10^{-1}	$5.3\times10^{-1}/O(1)$
δ^{23}	3.0×10^{-1}	$4.6\times10^{-1}/O(1)$

Table 8. Upper predictions on LFV decays of Z boson in MRSSM.

decay	prediction	future sensitivity [42-45]
$\mathrm{Br}(Z\to e\mu)$	$O(10^{-14})$	2.0×10^{-9}
$\mathrm{Br}(Z\to e\tau)$	$O(10^{-9})$	$(1.3-6.5)\times10^{-8}$
$\mathrm{Br}(Z\to \mu\tau)$	$O(10^{-9})$	$(0.44-2.2)\times10^{-8}$

tios of $Z\to l_i l_j$ equal zero. Considering the constraints from $l_2\to l_1\gamma$, we summarize the theoretical predictions of $Z\to l_1 l_2$ in MRSSM in Table 8, and the value is taken from Fig. 4 with M_D^W=600 GeV. The upper prediction on $\mathrm{Br}(Z\to e\mu)$ is seven orders of magnitude below current experimental bound, and we may make further efforts to observe it in a future experiment. The upper prediction on $\mathrm{Br}(Z\to e\tau)$ and $\mathrm{Br}(Z\to \mu\tau)$ are at the same order and close to the current experimental bound. Thus, the observations of LFV decays $Z\to e\tau$ and $Z\to\mu\tau$ may be more promising in a future experiment.

References

1 M. Tanabashi et al (Particle Data Group), Phys. Rev. D, **98**: 030001 (2018)
2 R. Akers et al (OPAL Collaboration), Z. Phys. C, **67**: 555 (1995)
3 G. Aad et al (ATLAS Collaboration), Phys. Rev. D, **90**: 072010 (2014)
4 M. Aaboud et al (ATLAS Collaboration), arXiv:1804.09568
5 P. Abreu et al (DELPHI Collaboration), Z. Phys. C, **73**: 243 (1997)
6 L. Calibbi, G. Signorelli, Riv. Nuovo Cim., **41**: 1 (2018)
7 G. D. Kribs, E. Poppitz, and N. Weiner, Phys. Rev. D, **78**: 055010 (2008)
8 P. Fayet, Nucl. Phys. B, **90**: 104 (1975)
9 A. Salam and J. Strathdee, Nucl. Phys. B, **87**: 85 (1975)
10 P. Diessner and W. Kotlarski, PoS CORFU, **2014**: 079 (2015)
11 P. Diessner, J. Kalinowski, W. Kotlarski, and D. Stöckinger, Adv. High Energy Phys, **2015**: 760729 (2015)
12 P. Diessner, J. Kalinowski, W. Kotlarski, and D. Stöckinger, JHEP, **1412**: 124 (2014)
13 P. Diessner, W. Kotlarski, S. Liebschner, and D. Stöckinger, JHEP, **1710**: 142 (2017)
14 P. Diessner, J. Kalinowski, W. Kotlarski, and D. Stöckinger, JHEP, **1603**: 007 (2016)
15 A. Kumar, D. Tucker-Smith, and N. Weiner, JHEP, **1009**: 111 (2010)
16 A. E. Blechman, Mod. Phys. Lett. A, **24**: 633 (2009)
17 G. D. Kribs, A. Martin, and T. S. Roy, JHEP, **0906**: 042 (2009)
18 C. Frugiuele and T. Gregoire, Phys. Rev. D, **85**: 015016 (2012)
19 J. Kalinowski, Acta Phys. Polon. B, **47**: 203 (2016)
20 S. Chakraborty, A. Chakraborty, and S. Raychaudhuri, Phys. Rev. D, **94**: 035014 (2016)
21 J. Braathen, M. D. Goodsell, and P. Slavich, JHEP, **1609**: 045 (2016)
22 P. Athron, J.-hyeon Park, T. Steudtner, D. Stöckinger, and A. Voigt, JHEP, **1701**: 079 (2017)
23 C. Alvarado, A. Delgado, and A. Martin, Phys. Rev. D, **97**: 115044 (2018)
24 K.-S. Sun, T.-F. Feng, T.-J. Gao, and S.-M. Zhao, Nucl. Phys. B, **865**: 486 (2012)
25 M. Aaboud et al (ATLAS Collaboration), Phys. Rev. D, **98**: 092012 (2018)
26 F. Staub, arXiv:0806.0538
27 W. Porod, F. Staub, and A. Vicente, Eur. Phys. J. C, **74**: 2992 (2014)
28 G. Passarino and M.J.G. Veltman, Nucl. Phys. B, **160**: 151 (1979)
29 H. H. Patel, Comput. Phys. Commun., **197**: 276 (2015)
30 A. Denner, S. Dittmaier, and L. Hofer, Comput. Phys. Commun, **212**: 220 (2017)
31 A. Denner and S. Dittmaier, Nucl. Phys. B, **658**: 175 (2003)
32 A. Denner and S. Dittmaier, Nucl. Phys. B, **734**: 62 (2006)
33 A. Denner, Fortsch. Phys., **41**: 307-420 (1993)
34 J. Rosiek, P. Chankowski, A. Dedes, S. Jager, and P. Tanedo, Comput. Phys. Commun., **181**: 2180 (2010)
35 A.M. Baldini et al (MEG Collaboration), Eur. Phys. J. C, **76**: 434 (2016)
36 B. Aubert et.al (BABAR Collaboration), Phys. Rev. Lett., **104**: 021802 (2010)
37 G.-J. Ding and M.-L. Yan, Phys. Rev. D, **77**: 014005 (2008)
38 J. Adam et al (MEG Collab.), arXiv:1301.7225
39 A. Crivellin, Z. Fabisiewicz, W. Materkowska, U. Nierste, S. Pokorski, and J. Rosiek, JHEP, **06**: 003 (2018)
40 M. Bona et al (SuperB Collab.), arXiv:0709.0451
41 P. Diessner, PhD thesis, Dresden, Tech. U., 2016
42 R. Benbrik and C.-K. Chua, Phys. Rev.. D, **78**: 075025 (2008)
43 J. A. Aguilar-Saavedra et al (ECFA/DESY LC Physics Working Group), arXiv:0106315
44 S. Heinemeyer, W. Hollik, A. M. Weber, and G. Weiglein, arXiv:0711.0456
45 J. Erler and P. Langacker, arXiv:0807.3023